

See discussions, stats, and author profiles for this publication at: <https://www.researchgate.net/publication/312379515>

Water body extraction from RapidEye images: An automated methodology based on Hue component of color transformation from RGB to HSV model

Article · June 2016

CITATIONS

3

READS

229

3 authors:



Laercio Namikawa

National Institute for Space Research, Brazil

44 PUBLICATIONS 263 CITATIONS

[SEE PROFILE](#)



Thales Sehn Körting

National Institute for Space Research, Brazil

124 PUBLICATIONS 304 CITATIONS

[SEE PROFILE](#)



Emiliano Ferreira Castejon

National Institute for Space Research, Brazil

20 PUBLICATIONS 282 CITATIONS

[SEE PROFILE](#)

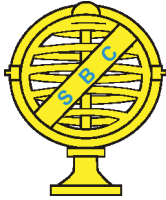
Some of the authors of this publication are also working on these related projects:



Burned areas mapping in Amazon rainforest using GEOBIA and Data Mining techniques [View project](#)



URBISAmazônia [View project](#)



WATER BODY EXTRACTION FROM RAPIDEYE IMAGES: AN AUTOMATED METHODOLOGY BASED ON HUE COMPONENT OF COLOR TRANSFORMATION FROM RGB TO HSV MODEL

Extração de Corpos d'Água Utilizando Imagens RapidEye: Metodologia Automatizada com Base no Componente Matiz da Transformação de Cores RGB para o Modelo HSV

Laércio Massaru Namikawa, Thales Sehn Körting & Emiliano Ferreira Castejon

**Brazil's National Institute for Space Research – INPE
Image Processing Division – DPI**

Av. dos Astronautas, 1758 São José dos Campos, Brazil
{laercio, thales, castejon}@dpi.inpe.br

*Received on December 17, 2015/ Accepted on February 27, 2016
Recebido em 17 de Dezembro, 2015/ Aceito em 27 de Fevereiro, 2016*

ABSTRACT

Water management and flood studies are some fields in which a map with all water bodies in a region is useful, especially in scenarios of environmental changes due to anthropogenic factors. Various detection methods of water body surfaces in remotely sensed images are available, from simple methods having a lower accuracy to more sophisticated ones. The objective of this paper is to present a simple, yet accurate method to detect water bodies in RapidEye images. The motivation is the availability of country wide coverage of these images, which makes feasible the generation of a map of all water bodies detectable at that spatial resolution. Our solution is the use the color transformation from Red-Green-Blue to Hue-Saturation-Value and the minimum radiance from all RapidEye bands to classify water bodies in seven classes of water. The water classes are ranked based on the confidence of the classified pixels being water, which accommodates for the differences in illumination and scattering that are present in such a large coverage, composed by more than 15000 scenes. In addition, users of the generated water bodies map can reclassify based on their needs. The methodology was developed on two RapidEye scenes, covering the Jacareí and Foz do Iguaçu municipalities, in Brazil. Results indicate that the classification is better than the traditional ones, with the advantage of providing seven classes with confidence levels.

Keywords: RapidEye, Water Body Detection, RGB-HSV Color Transformation.

RESUMO

Gerenciamento de bacias hidrográficas e estudos sobre enchentes são exemplos de casos onde é útil a existência de um mapa contendo todos os corpos d'água de uma região, especialmente em cenários de mudanças ambientais abruptas, devido a fatores antropogênicos. Existem vários métodos de detecção de superfícies de corpos d'água utilizando imagens de sensoriamento remoto, desde os mais simples contendo baixa acurácia até os mais sofisticados. O objetivo deste trabalho é apresentar um método que combine uma taxa de acerto adequada a uma metodologia simples, para ser aplicado em imagens do satélite RapidEye. A motivação para a gerar este método foi a disponibilidade de uma cobertura completa do Brasil com imagens RapidEye. Esta base de imagens permite a descoberta de corpos d'água detectáveis através da resolução espacial do RapidEye. Para isso, deve-se aplicar a transformação de cores RGB (siglas em inglês

para vermelho, verde e azul) para o modelo de cores HSV (matiz, saturação e valor). Além disso, foram incluídos os valores de mínima radiância das 5 bandas do RapidEye para classificar os corpos d'água em um ranqueamento de sete classes de pertencimento ao alvo de interesse (Água). Esta solução é adaptável aos diferentes tipos de iluminação e espalhamento presentes em uma grande cobertura de imagens, como neste caso da cobertura do Brasil com mais de 15000 cenas RapidEye. Além disso, potenciais usuários do produto gerado por esta proposta podem reclassificar o mapa conforme a necessidade, removendo classes de menor pertencimento, por exemplo. A metodologia foi desenvolvida a partir da análise de duas cenas RapidEye. Uma delas cobre o município de Jacareí, São Paulo, e a outra cobre Foz do Iguaçu, no Paraná. Os resultados obtidos indicam que a classificação é superior aos métodos tradicionais, com a vantagem de apresentar as sete classes de pertencimento.

Palavras chaves: RapidEye, Detecção de Corpos d'Água, Transformação de Cores RGB para HSV.

1. INTRODUCTION

The use of water bodies detection method on remote sensed images is useful in many different applications, from water management and flood studies to changes in water availability due to anthropogenic factors. Water bodies are characterized by low reflectance, with decrease of the reflectance as the wavelength increases in optical multispectral images. Existing methods to extract the surface of the water bodies are based on methods from simple thresholding images to sophisticated classification schemes based on spectral and shape attributes. Simple methods use thresholding of individual bands or a ratio between two bands to enhance the low reflectance areas. The simplicity of these methods has drawbacks related to the confusion with other low reflectance targets, such as shadows, asphalt cover and dark soils. Sophisticated methods which employ statistical and knowledge based classification schemes can improve results with the additional cost of computational power and with the requirement for user interaction.

The motivation of developing a new method to detect water bodies surfaces is to create a country wide map of water bodies at a 5 meter resolution. The source of information is composed by RapidEye images from the Brazilian Environmental Ministry Geo Catalog, which has made available the full coverage of Brazil with RapidEye multispectral imagery (MMA, 2016). RapidEye images are generated from a constellation of 5 satellites located at the same orbital plane, and carrying the same sensors (BLACKBRIDGE, 2015). Available RapidEye imagery are processed into level 3A, which corresponds to geometric, radiometric and sensor correction, and mosaicked into 25

by 25 km tiles with a 5 meter pixel size, created from the acquisition sampled at 6.5 meters at the nadir. The multispectral bands are 5: blue (0.44 to 0.51 μm), green (0.52 to 0.59 μm), red (0.63 to 0.685 μm), red edge (0.69 to 0.73 μm), and Near Infra-Red - NIR (0.76 to 0.85 μm). Digital numbers in each RapidEye band are the radiance collected at the sensor in 12-bit and converted into 16 bit integer values corresponding to 1/100 of radiance in $\text{W}/\text{m}^2 \text{sr } \mu\text{m}$.

A nationwide coverage using RapidEye tiles implies that there are more than 15000 multispectral (5 band with 16 bit each) images to be processed to detect water bodies. This amount of data to be processed requires the water body detection to be fast and independent of expert inputs. Therefore, the choice here is for a method with simple band operations with global thresholds.

2. RELATED WORK

The analysis of water reflectance curves indicates that water bodies can be separated from other non-water features in a simple way due to its lower reflectance when compared to the reflectance of other non-water targets. However, in real world interactions of water with suspended sediment type and concentration, in water vegetation (submerged vegetation, algae and macrophytes), water depth, bottom substrate and morphology, among other factors alter the reflectance of water bodies.

Considering that clear, deep water reflectance is low in optical wavelengths and is lower in infrared (BOWKER *et al.*, 1985), the simplest method is the use of thresholding of the band with the lowest reflectance. For Landsat 5 TM data, Frazier *et al.* (2000) found that thresholding of the band 5 (SWIR 1.55

to 1.75 μm) produces similar results to the maximum-likelihood classification, with the later underestimating water pixels and the thresholding including false positive pixels. The band 4 (NIR) was similar to band 5, with a tendency to include more commission errors (pixels that are not water) from poor pasture, hill shadow and parts of urban area.

The rationing of two bands is an image enhancing technique that minimizes the effects due to differences in illumination, which could make the use of one band thresholding not reliable when using a single threshold value for a set of images. In addition, the use of an index similar to the Normalized Difference Vegetation Index (NDVI) with appropriate bands, has the potential to define water and non-water pixels based on positive or negative values of the index.

For detection of water bodies, McFeeters (1996) proposed the Normalized Difference Water Index (NDWI), to enhance the reflectance difference between a visible (red or green) band from the NIR band for water features when compared to vegetation and soils. NDWI is the ratio between the difference and the sum of the green band and the NIR band. Water features will have values greater than zero, which is the threshold to be used in the method, since the difference for water reflectance is greater than the difference for soils and vegetation.

XU (2006) proposed a modification to NDWI in order to minimize the noise from built-up areas, which exists because the built-up areas have a similar reflectance to water in green and NIR bands when absolute values are not considered. Since the reflectance of middle infra-red radiation is higher in built-up areas when compared to the NIR radiation, XU (2006) modified NDWI (MNDWI) to use the middle infra-red band instead of the infra-red one.

Another technique that overcomes the illumination effects required to specify a simple method to extract water bodies from multiple images is the use of color information. In our previous research, we detected water bodies based on the Hue component from a color transformation (NAMIKAWA, 2015). When comparing histograms using NDWI, MNDWI and Hue component from the Red-Green-Blue (RGB) composition with the middle infra-red,

NIR and red bands from Landsat 8, we obtained fewer pixels in the confusion region between the values for water and non-water in the Hue component when compared to the NDWI and MNDWI ratios.

In this study, we propose the use of thresholding of the Hue component of the conversion of color system from RGB to Hue-Saturation-Value (HSV) as a better solution when compared to the use of a single band thresholding and the use of NDWI. The RGB color model is based on a cube defined on a Cartesian coordinate system, with one of the vertices of the cube at the origin and three of the edges running along the three axes of the coordinate system. The axes values are associates with intensities of Red, Green and Blue colors. The HSV color model uses a cylindrical coordinate system, with the vertical axis (running along the center of the cylinder) defining the Value component, the perpendicular distance from the vertical axis defining the Saturation component, and the Hue component being measured as the angle around the vertical axis. The zero angle of the Hue component corresponds to red color, followed by yellow at 60°, green at 120°, cyan at 180°, blue at 240°, magenta at 300° and back to red at 360°. More details about color models can be found in FOLEY *et al.* (1996).

3. METHODOLOGY FOR WATER BODIES DETECTION

The methodology used here to define the best method using the Hue component of the RGB to HSV conversion is to obtain results from the traditional methods, test all possible RGB compositions of RapidEye, select the best RGB and compare with the traditional methods results to verify if the proposed method is better. Testing and comparison requires a set of known classification of water bodies and non-water features. Therefore, two RapidEye tiles were selected based on the amount of different targets, with a substantial quantity of water bodies, and also on the author's local knowledge. Most of the first tile covers the Jacareí municipality in São Paulo state (tile from October 10, 2014 named 2328310 in the RapidEye reference framework) and the second tile covers the Foz do Iguaçu municipality in Paraná state (tile from August 08, 2014 named

2127325 in the same framework), as shown in Fig. 1. All figures in this paper presenting images derived from Jacareí and Foz do Iguaçu images are map projected to the coordinate system as shown in Fig. 1.

To obtain the results presented in this article we used *SPRING* version 5.3 free open source software, available at <http://www.spring-gis.org/> (CAMARA *et al.*, 1996).

The identification of water bodies in both images by automatic classification method provided the basis for the tests of the simple thresholding methods. The supervised classification option was discarded given that the amount of samples for the small water bodies is reduced when compared to large water bodies, therefore this could skew the classification

We employed the automatic K-Means classifier, which is an implementation of the initial arbitrary cluster centers algorithm (LLOYD, 1982). We used K equal to 10, run the

algorithm for 10 iterations, on the 5 bands of the RapidEye images. The resultant classifications from Jacareí and from Foz do Iguaçu images are shown in Fig. 2.

The visual analysis of the unsupervised classification results in Fig. 2 and the author's knowledge of the areas indicate that most water bodies are presented in red color in the classification results from both images. The yellow color represents most dark areas, such as shadows, asphalt, burn scars and dark soils. Other colors represent the remaining features, such as vegetation, soils, and built-up areas. The analysis of the areas classified as water bodies indicate that there are commission errors where dark soils and shadows are misclassified as water. The omission errors occur where water bodies are shallow or have a high sediment concentration. Some of the misclassification was manually corrected to be used in the following steps.

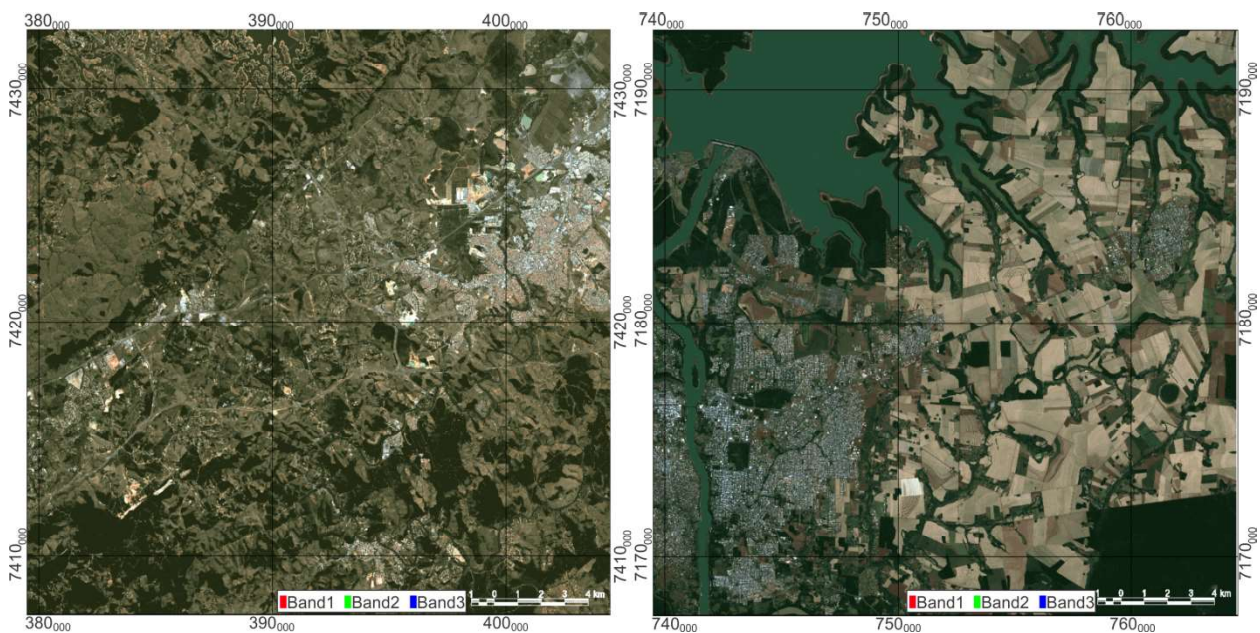


Fig. 1 - Selected images in R3G2B1 enhanced color composition with UTM projection in Datum WGS-84. Left image is over Jacareí, with UTM zone 23 south and right image is over Foz do Iguaçu, with UTM zone 21 south.

The first traditional method to be tested is the thresholding of an Infra-Red band. For RapidEye images, the band 5 (NIR, 0.76 to 0.85 μm) has similar wavelengths to Landsat 5 band 4 (0.76 to 0.90 μm), which is the second best option for Landsat 5 images (FRAZIER *et al.*, 2000). The water bodies in the images were used to find the thresholding level for RapidEye band

5 by analyzing the distribution of the reflectance of pixels detected as water body in the K-Means classification image and of pixels detected as from non-water features. The histograms are presented in Fig. 3.

The interval analysis of the distribution of water body pixel values in Jacareí image (Fig.3 left) indicates that 75% of the water pixels are

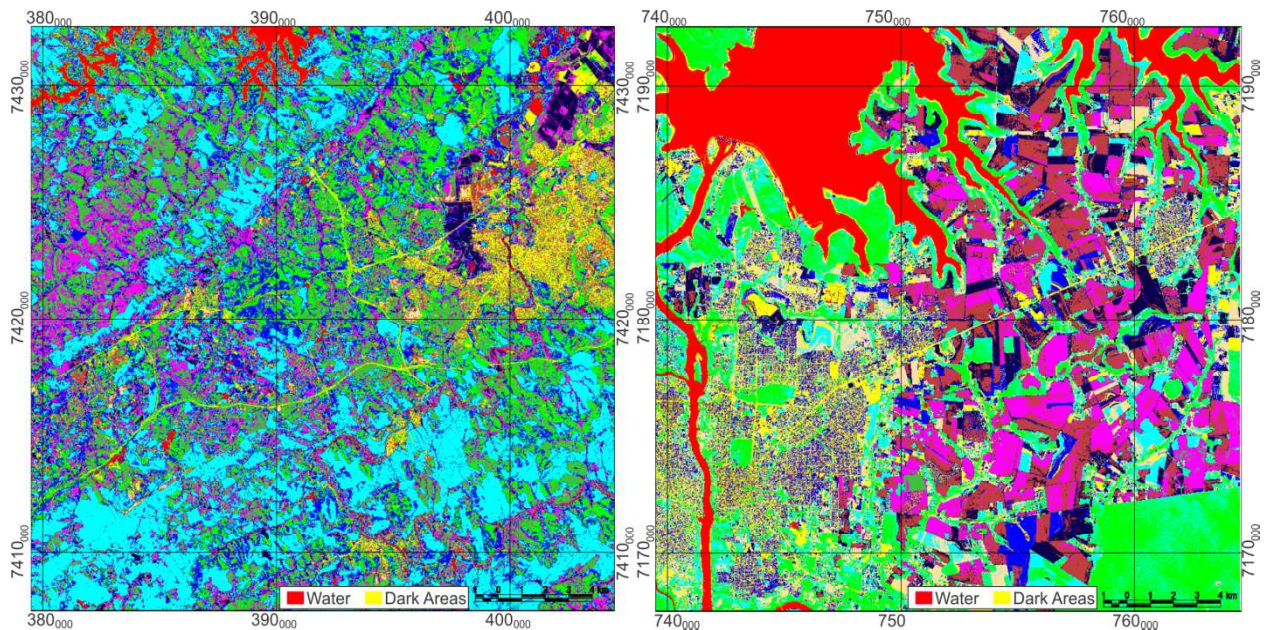


Fig. 2 - Unsupervised classification results using K-Means for both test areas shown in Fig. 1. We used $K = 10$, and 10 iterations each execution. Water bodies are presented in red color in both results and yellow color represents dark areas. Other colors represent other types of features.

below 2500, 90% are below 3500 and 99.9% are below 5000. The interval analysis of the distribution of non-water pixel values in the same image indicates that 0.05% of the non-water pixels are below 3000, 0.2% are below 3800 and 1% are below 5000. For the Foz do Iguazu band 5

image, 75% of the water pixels are below 1100, 90% are below 1300 and 99.9% are below 3000. The interval analysis of the distribution of non-water pixel values in the same image indicates that 0.05% of the non-water pixels are below 2000, 0.2% are below 2500 and 1% are below 3000.

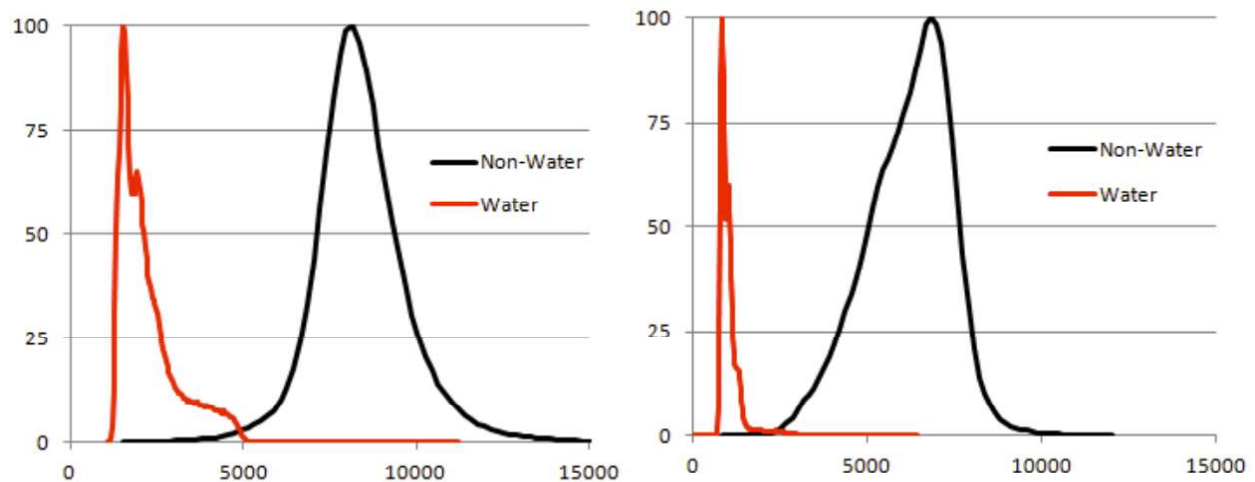


Fig. 3 - Histograms of RapidEye band 5 of Jacareí (left) and Foz do Iguazu (right) images, highlighting pixels detected as Water (in red) versus other classes (Non-Water).

Based on the analysis of the reflectance values distribution for water and non-water pixels, the following general thresholds were applied on both images: Class WATER to digital levels 0 to 2000, Class WATER95 to digital levels 2000 to 2500, Class WATER90 to digital

levels 2500 to 3000, Class WATER80 to digital levels 3000 to 4000, and Class WATER70 to digital levels 4000 to 5000.

The visual analysis of the RapidEye band 5 image classification results indicates that for both images, omission errors for water pixels class are

not found easily, but there are many commission errors, as expected in dark targets, such as shadow, asphalt pavement and dark soils. In addition, the water pixels are classified in all five water classes. Fig. 4 shows a portion of the Jacareí image where illumination effects on reservoir water produces four classes of water. Fig. 5 shows part of the Foz do Iguaçu image with the Paraná River and the cities of Foz do Iguaçu - Brazil and Ciudad del Leste - Paraguay, where built-up features are misclassified in all five classes of water.

The test of the classification based only on the RapidEye band 5 image thresholding indicates that it is not a reliable solution, given that the sensitivity to illumination effects requires the use of classes that will include built-up features pixels.

The second method to be tested is the thresholding of the Water Index, as proposed by (MCFEETERS, 1996) and (XU, 2006), which minimizes the illumination effects. RapidEye images do not have the middle infrared band, therefore the detection method tested here is the NDWI using the NIR (0.76 to 0.85 μm) band 5 and threshold equal to zero. The Jacareí and Foz do Iguaçu bands 2 and 5 were used to create de NDWI images. The radiance of the bands were first normalized based on the exo-atmospheric irradiance for each band and then the ratio of normalized bands 2 (NB2) and 5 (NB5) was created using $(\text{NB2} - \text{NB5}) / (\text{NB2} + \text{NB5})$. The histograms of the NDWI images for water and non-water pixels from the edited K-Means classification are shown in Fig. 6.

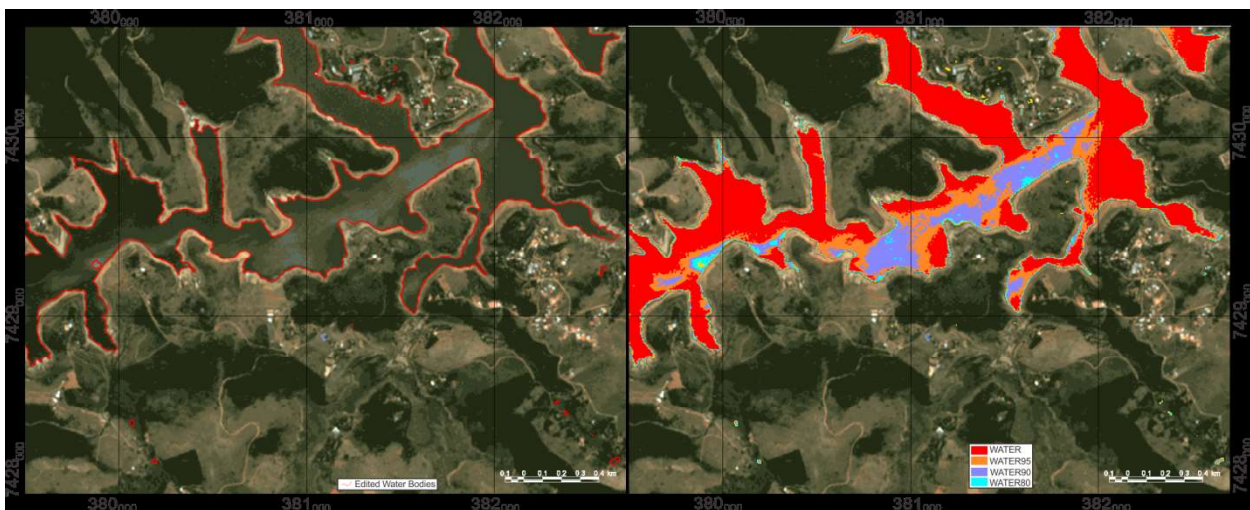


Fig. 4 - A portion of the Jacareí image, with the R3G2B1 enhanced color composition overlaid by the edges of the reservoir from the K-Means classification (left), and the classification result from the band 5 thresholding (right).

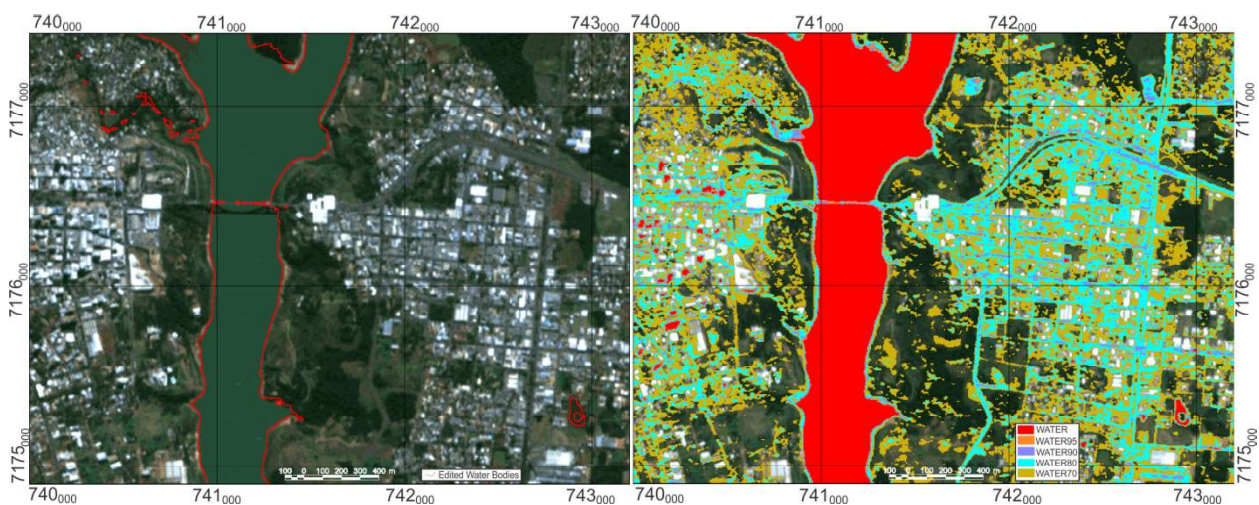


Fig. 5 - A portion of the Foz do Iguaçu image, with the R3G2B1 enhanced color composition overlaid by the edges of the Paraná River and an urban lake from the K-Means classification (left), and the classification result from the band 5 thresholding (right).

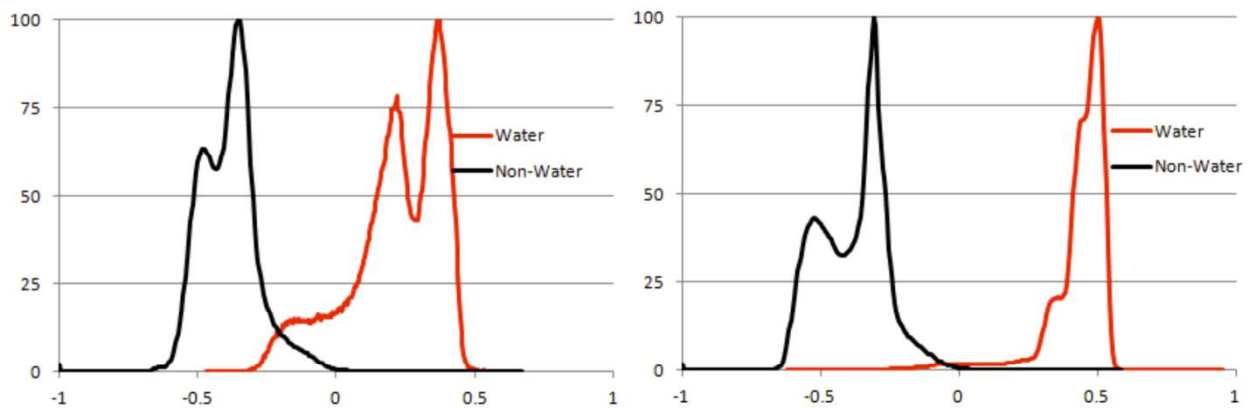


Fig. 6 - Histograms of RapidEye NDWI of Jacareí (left) and Foz do Iguazu (right) images, highlighting pixels detected as Water (in red) versus other classes (Non-Water).

Fig. 6 indicates that all non-water pixel values are below zero and that some water pixels are below zero. In Foz do Iguazu image, 99.9% of non-water pixels have NDWI values below zero and 2% of water pixels have NDWI below zero. For Jacareí image, 99.8% of non-water pixels have NDWI values below zero and 13.2% of water pixels have NDWI below zero. These results indicate that there are pixels of non-water misclassified as water pixels and pixels of water that will not be correctly classified with the NDWI zero threshold.

The threshold of zero, that is, all pixels with NDWI values higher than zero are water bodies,

was applied to the NDWI images from Jacareí and Foz do Iguazu. A close analysis of both results indicates that most water bodies are detected by the zero threshold on NDWI images. However, there are also shadows, dark pavement and high reflectance urban features included in the detected pixels. Fig. 7 shows that some small areas with water pixels are missing in the classification using the NDWI thresholding, some water pixels that were detected by the K-Means classification were detected, and some pixels from built-up features are misclassified as water pixels. Fig. 8 presents an example of the misclassification of shadows as water, where the Itaipu Dam casts shadows.



Fig. 7 - A portion of the Jacareí image, with the R3G2B1 enhanced color composition overlaid by the edges of the Paraíba do Sul River and sand mining lakes from the K-Means classification (left), and the classification result from the NDWI thresholding (right).

Finally, to define and compare the proposed method based on the Hue component from a color transformation, the Hue components of the transformation from Red-Green-Blue (RGB)

color model to the Hue-Saturation-Value (HSV) color model were calculated from correspondent band combinations of the RapidEye 5 bands using a program written in *LEGAL* language,

available in *SPRING* software. The *LEGAL* program is based on the algorithm described by (FOLEY *et al.*, 1996). The algorithm requires the RGB information to be in the 0 to 1 range; therefore, all RapidEye 5 bands were converted to their normalized radiance values using the exo-atmospheric irradiance for each band, presented in the image specification (BLACKBRIDGE, 2015).

The RapidEye 5 bands used to create the RGB combination were (Color-Band number): R1G2B3; R1G2B4; R1G2B5; R1G3B4; R1G3B5; R1G4B5; R2G3B5; R2G3B5; R2G4B5; and R3G4B5. Other combinations of

different bands would create Hue components similar to one of the previous (the differences would be in the inversion and translation of the initial values), therefore we did not test them.

To select the best Hue component to separate water from non-water targets, the area from Fig. 9 was selected in the Foz do Iguaçu image, given that it contains a comparable quantity of water bodies, urban areas and vegetation targets, providing a good sample set for the statistical analysis. The Hue components are presented in Fig. 10 by the histograms from water only pixels and non-water features pixels.



Fig. 8 - A portion of the Foz do Iguaçu image, with the R3G2B1 enhanced color composition overlaid by the edges of the Paraná River and the Itaipu reservoir from the K-Means classification (left), and the classification result from the NDWI thresholding (right).



Fig. 9 - Region of of the Foz do Iguaçu image used to collect the sample set for the statistical analysis.

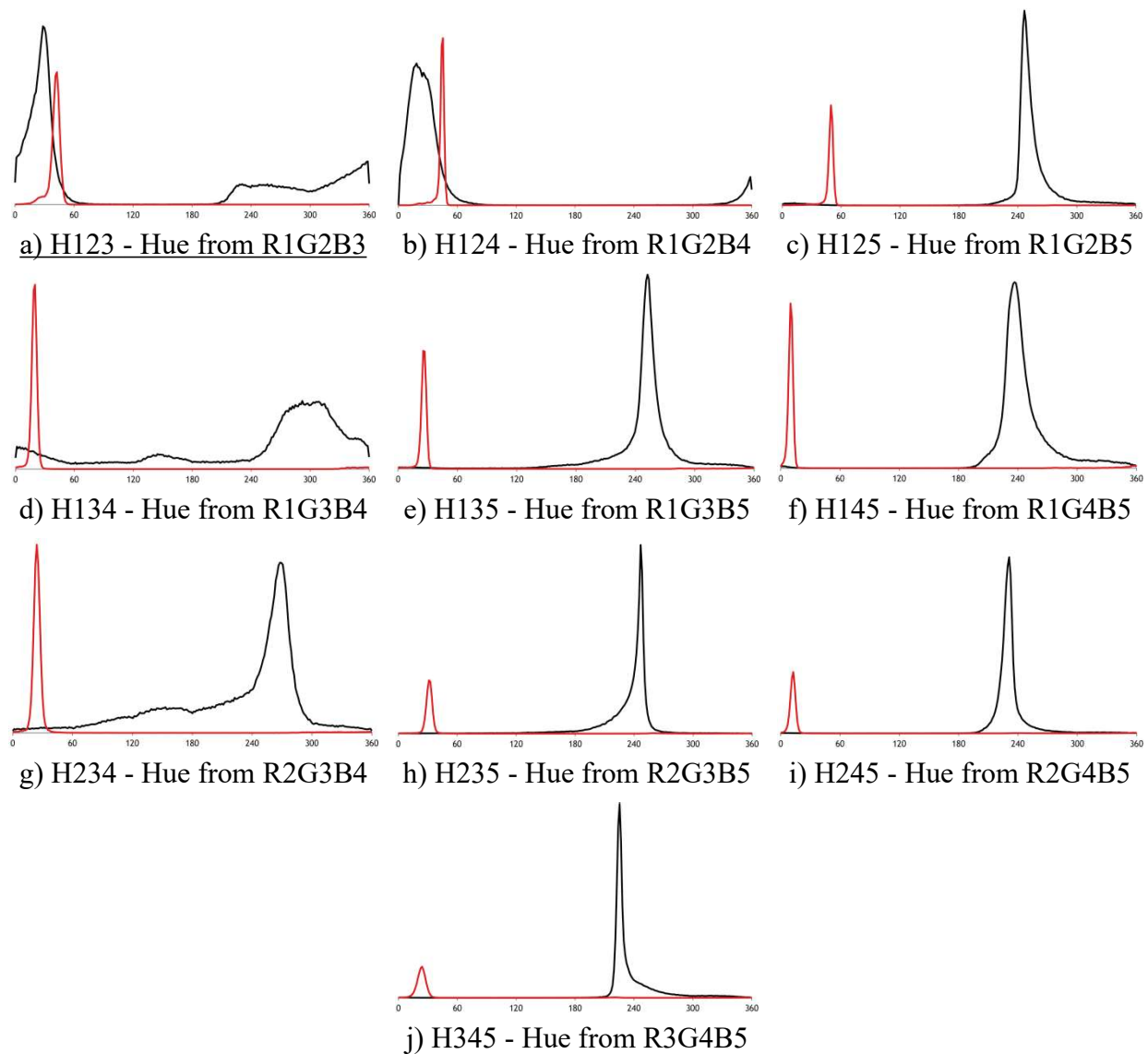


Fig. 10 - Comparison between Hue components obtained by different combinations of Rapideye bands. Red color indicates the histogram of pixels classified as Water in the K-Means classification and black color represents the histogram of pixels classified as Non-Water.

A visual analysis of the Hue components in Fig. 10 can be executed to define if there is confusion between the water and non-water classes and be based on the separation being possible if the intersection of the histograms is empty or near empty. The analysis indicates that Hue component from color compositions R1G2B3, R1G2B4, R1G3B4 and R2G3B4 do not separate water from non-water features and the other 6 compositions do separate them.

To classify the remaining Hue components which are candidates for the best one to separate water features from non-water targets, a percentile analysis based on 90, 95 and 98

percentages was executed. From the histograms, the range of Hue values associated to the first 90%, 95% and 98% of water pixels was defined for each Hue component. Likewise, the range of Hue values associated to the first 90%, 95% and 98% of non-water pixels was also defined. This range of Hue values is presented in Table 1. Note that Hue values are circular, from 0 degrees to 360 degrees, with 0° (and 360°) representing red, 120° green and 240° blue colors.

Next, the number of pixels of non-water inside each one of the percentiles for water pixels was counted and, in a similar way, the number of pixels of water inside each one of the percentiles for non-water pixels was also

counted. The misclassified pixels were converted into percentage of the total pixels of their classes, that is, for example what percentage of water pixels fall inside the Hue values range 90, 95

and 98% of non-water pixels. Table 2 shows the number of pixels and the percentage inside parenthesis from the total number of pixels in the class.

Table 1: Hue values of RapidEye bands combinations for each percentile range

Hue from color composition	Water			Non-Water		
	90%	95%	98%	90%	95%	98%
R1G2B5	32° - 52°	10° - 52°	308° - 53°	238° - 283°	228° - 319°	218° - 4°
R1G3B5	9° - 28°	345° - 29°	306° - 30°	199° - 284°	180° - 323°	161° - 12°
R1G4B5	0° - 12°	345° - 13°	310° - 14°	218° - 283°	211° - 313°	205° - 340°
R2G3B5	16° - 35°	324° - 36°	308° - 37°	197° - 251°	178° - 260°	160° - 33°
R2G4B5	0° - 15°	323° - 16°	249° - 17°	215° - 246°	211° - 263°	205° - 309°
R3G4B5	357° - 28°	228° - 30°	215° - 33°	220° - 267°	218° - 298°	214° - 330°

Table 2: Misclassified number of pixels and percentage (inside parenthesis) from total for hue components of RapidEye bands combinations for each percentile range

Hue from color composition	Non-Water Pixels in Water Percentile Range			Water Pixels in Non-Water Percentile Range		
	90%	95%	98%	90%	95%	98%
R1G2B5	992 (0.37%)	3773 (1.41%)	16145 (6.02%)	199 (0.44%)	527 (1.17%)	1012 (2.24%)
R1G3B5	1446 (0.54%)	4460 (1.66%)	14540 (5.42%)	92 (0.20%)	691 (1.53%)	2497 (5.53%)
R1G4B5	862 (0.32%)	3861 (1.44%)	15288 (5.70%)	198 (0.44%)	509 (1.12%)	920 (2.04%)
R2G3B5	511 (0.19%)	1900 (0.71%)	2633 (0.98%)	52 (0.12%)	345 (0.76%)	33658 (74.52%)
R2G4B5	238 (0.20%)	3547 (1.32%)	23313 (8.69%)	437 (0.97%)	685 (1.52%)	992 (2.20%)
R3G4B5	886 (0.33%)	127582 (47.55%)	265274 (98.86%)	722 (1.60%)	971 (2.15%)	1367 (3.72%)

Considering that the 98 percentile has a large range of percentage values, from 0.98% to 98.86%, the 90 and 95 percentiles were arbitrarily selected to define an index, which is the sum of the percentages of misclassified pixels for each Hue component. Table 3 presents the percentages and the calculated index to used to select the best Hue component to separate water from non-water features is the one from the R2G3B5 color composition.

The definition of the threshold of water features was also based on the percentile analysis. To be able to execute further analysis,

four different classes were created with three thresholds. The first class is named WATER and its Hue thresholds are taken from the 90 percentile for water pixels. The second class is WATER95, with thresholds from the 95 percentile Hue values range for water pixels, excluding the already used 90 percentile. The third class is WATER90, using the 98 percentile Hue values for water pixels, excluding the Hue values already associated to the other classes. Finally, the fourth class WATER80 thresholds are from non-water 98 percentile, using the Hue values that represent the 2% of non-water values.

Table 4 shows the range of Hue values for each one of the classes, including the range values for compositions which are not the best (R2G3B5 color composition).

The thresholds were applied to the respective Hue components using a program written in *LEGAL* language from *SPRING* software. A visual analysis of the resulting classifications indicates that the Hue component from the

R2G3B5 color composition is better than the other ones, confirming the rank defined by the Index in Table 3. Fig. 11 shows the comparison of the classification using the MNDWI and the other one using the Hue component from the R2G3B5 color composition for an area in Jacareí image, indicating that the classifications are similar. Fig. 12 presents the same the comparison for a portion of Foz do Iguacu Jacareí image.

Table 3: Percentage from total of misclassified number of pixels for hue components of RapidEye bands combinations and the ranking index

Hue from color composition	Non-Water in Water		Water in Non-Water		Index
	90%	95%	90%	95%	
R1G2B5	0,37%	1,41%	0,44%	1,17%	3.39
R1G3B5	0,54%	1,66%	0,20%	1,53%	3.93
R1G4B5	0,32%	1,44%	0,44%	1,12%	3.32
R2G3B5	0,19%	0,71%	0,12%	0,76%	1.78
R2G4B5	0,20%	1,32%	0,97%	1,52%	4.01
R3G4B5	0,33%	47,55%	1,60%	2,15%	51.68

Table 4: Range of hue values for each class

Hue from color composition	WATER	WATER95	WATER90	WATER80
R1G2B5	32° - 52°	10° - 32°	308° - 10° and 52° - 53°	53° - 218°
R1G3B5	9° - 28°	28° - 29° and 345° - 9°	29° - 30° and 306° - 345°	30° - 161°
R1G4B5	0° - 12°	12° to 13° and 345° - 0°	13° - 14° and 310° - 345°	14° - 205°
R2G3B5	16° - 35°	35° - 36° and 324° - 16°	36° - 37° and 308° - 324°	37° - 160°
R2G4B5	0° - 15°	15° - 16° and 323° - 0°	16° - 17° and 249° - 323°	17° - 205°
R3G4B5	357° - 28°	28° - 30° and 228° - 357°	30° - 33° and 215° - 228°	33° - 214°

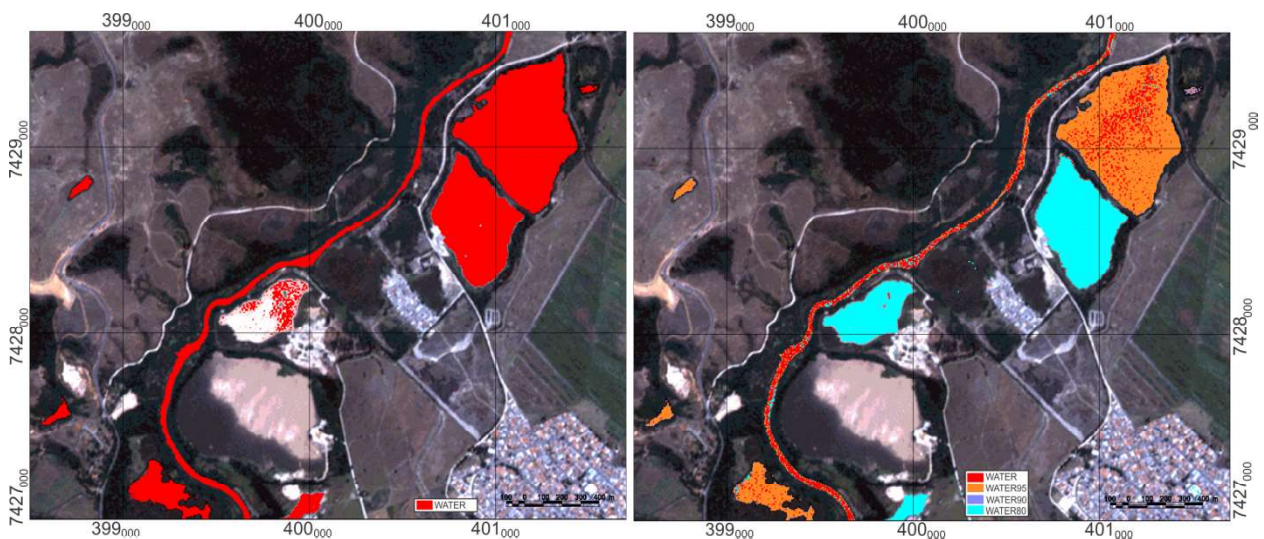


Fig. 11 - Comparison between classification using MNDWI (left) and using Hue component from the R2G3B5 color composition (right) for an area in Jacareí image.



Fig. 12 - Comparison between classification using MNDWI (left) and using Hue component from the R2G3B5 color composition (right) for a region in Foz do Iguaçu image.

In the classification using the Hue component from both images, in high reflectance urban features, the method has commission errors, which is a characteristic of NDWI (XU, 2006). If one considers the hypothesis that these high reflectance built-up areas have a minimum reflectance in all bands that has a very low probability, due to the relatively few such features in the image, then the method can be improved by rejecting the areas detected as water bodies but which have a minimum reflectance that is above a value defined according to a statistical analysis as being with very low probability. Assuming a cumulative distribution of minimum reflectance in all bands, one can accept the 99.5% of the pixels and reject the 0.5% pixels with the highest reflectance. Applying this assumption, all pixels that were previously detected as water will be rechecked and should have a minimum reflectance not greater than the value which defines the upper 0.5% of pixels in the cumulative distribution to be classified as water pixel.

In addition, the cumulative distribution of minimum reflectance in all bands can also be used to create different classes based on other percentiles to allow finer analysis of the extracted water features. The first 3 classes are the same as defined based on the Hue component 90%, 95% and 98% percentiles with the restriction based on minimum reflectance added. The other three classes were based arbitrarily on the 90%, 95%

and 99% percentiles, and on the Hue component cumulative distribution of non-water features, which was defined as WATER80.

The class WATER80 is now defined as with the pixels which were not classified in WATER, WATER95 and WATER90, with Hue thresholds taken from the 98% percentile of non-water pixels, and with a minimum reflectance lower than the 90% percentile of the cumulative distribution of minimum reflectance in all bands. Class WATER70 will be associated to pixels not yet classified, with the same Hue thresholds as WATER80 and belonging to the 95% percentile of the cumulative distribution. Class WATER60 will have the pixels with the same restriction for Hue value as WATER70 and WATER80, not classified yet, and with minimum reflectance values lower than the 99% percentile of the cumulative distribution. Finally, the class WATER50 will have the pixels with the same restriction for Hue value as WATER60, not yet classified and with minimum reflectance values lower than the 99.5% percentile of the cumulative distribution.

The omission errors that are present when the previous threshold defined by the cumulative distribution of the minimum reflectance is used are from water with suspended sediment in high quantity. Although a typical reflectance of turbid water is below 10% (BOWKER et al, 1985), high concentrations of sediment can increase water reflectance by a positive high

correlation with the sediment concentration (NOVO *et al.*, 1989).

Since the thresholds extracted from the cumulative distribution are used to classify water features in classes defined by statistical analysis, it is considered that these classes have arbitrary bounds and the classes must be carefully analyzed by the user of the information in accordance to the intended application of the water bodies map. Therefore, in this method the cumulative distribution of minimum reflectance in all bands the pixels from non-water targets in the Foz do Iguacu image (accordingly to the

edited K-Means classification) was used.

For Foz do Iguacu image, the radiance of all bands were normalized based on the exo-atmospheric irradiance for each band and the lowest value for each pixel was defined as the minimum normalized radiance (MNR). The statistical analysis of the MNR for the Non-Water features indicate that 99.5% of pixels have MNR below 0.425, 99% of pixels MNR values are below 0.375, 95% 0.335, and 90% of 0.320. Table 5 presents these values and the classes definition based on Hue and MNR thresholds.

Table 5: Range of hue values and minimum normalized radiance for each class

	WATER	WATER95	WATER90	WATER80	WATER70	WATER60	WATER50
Hue from R2G3B5 composition	16° - 35°	35° - 36° / 324° - 16°	36° - 37° / 308° - 324°	37° - 160°	37° - 160°	37° - 160°	37° - 160°
MNR	0 - 0.475	0 - 0.475	0 - 0.475	0 - 0.320	0.320 - 0.335	0.335 - 0.375	0.375 - 0.475

The 0.425 value is within the expected maximum range for water reflectance (would be equivalent to 42.5%), even if the true reflectance was calculated taking into account the solar incidence angle and the scattering effects. It must be noted that misclassification will occur if there are strong effects from sun glare and haze, which will scatter energy and add to the reflected radiance.

The application of the MNR threshold values on the classification of the Hue component from the R2G3B5 color composition was applied using a program written in *LEGAL* language from *SPRING* software. Fig. 13 shows a comparison with the classification considering the MNR threshold in the Jacareí image and Fig. 14 presents the same comparison for the Foz do Iguacu image. In both images the commission errors are reduced, with some left at built-up areas, mostly due to shadows.

4. CONCLUDING REMARKS AND FUTURE DIRECTIONS

The technique presented in this paper fulfills the requirement defined to detect all water bodies surfaces from the country wide

coverage of RapidEye images using a simple method that does not require user intervention and with little computational power. The method consists in three steps: 1) transformation from the RGB to HSV color model; 2) comparison to find the minimum normalized radiance (MNR) from all bands; 3) thresholding that combines values from the Hue component of the color model transformation and the values from the MNR, delivering seven classes of confidence in being a water body.

The analysis of the classification using the technique for the two images (Jacareí and Foz do Iguacu) indicate that the water bodies detection method using the Hue component from the R2G3B5 color composition and the MNR is similar to the traditional NDWI method. In addition, the thresholding in different confidence classes provided the user with flexibility to reclassify and edit the resulting map to remove errors due to noise and confusion with shadows and built-up areas. The seven confidence classes accommodate the differences that occur when using a common threshold for the huge amount of images present in country wide coverages.

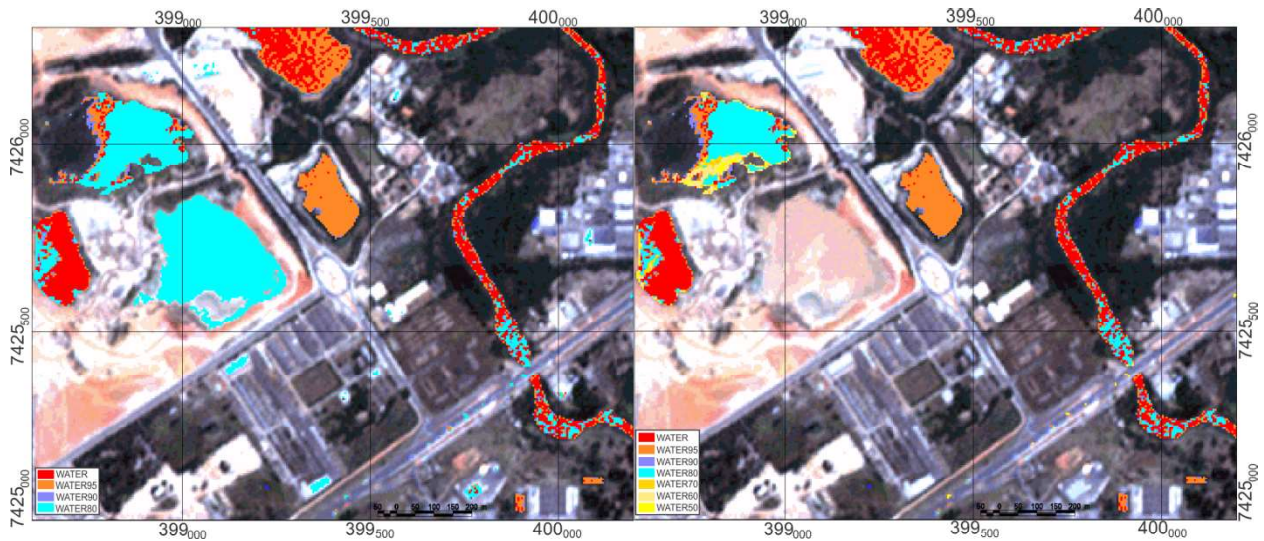


Fig. 13 - Comparison between classification using Hue component from the R2G3B5 color composition only (left) and adding MNR threshold values for a region in Jacareí image (right).

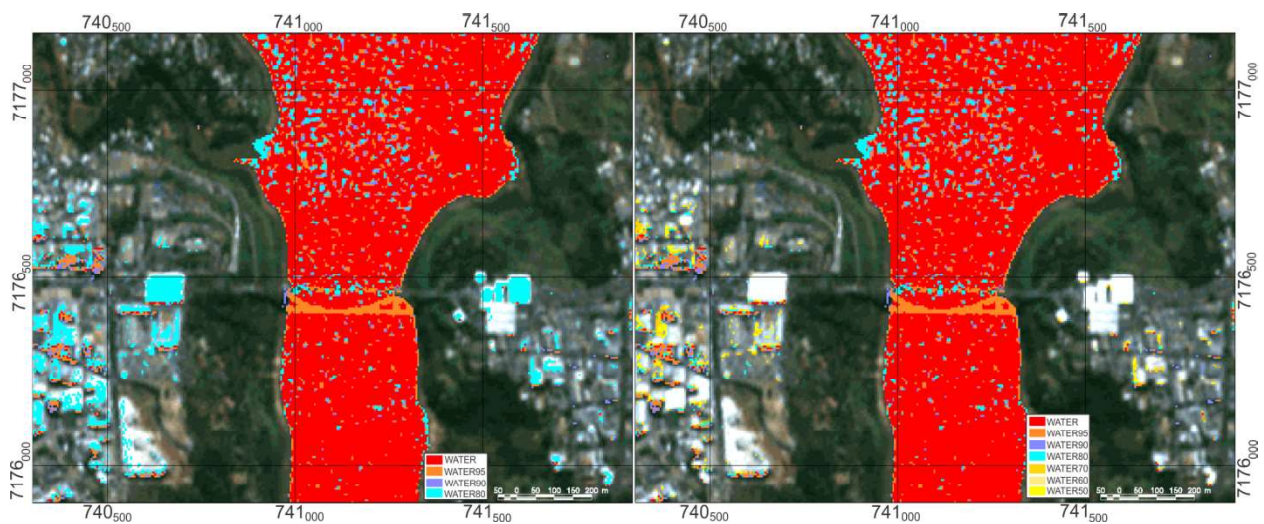


Fig. 14 - Comparison between classification using Hue component from the R2G3B5 color composition only (left) and adding MNR threshold values for a region in Foz do Iguaçu image (right).

In this implementation, the *LEGAL* language was used to program the three steps in the *SPRING* software. Although, the implementation is executed in a reasonable time, to process the whole set of RapidEye images, a C++ language program is being created using the TerraLib Version 5 open source GIS software library (available from: <http://www.dpi.inpe.br/terralib5/>). The new implementation will also generate a vector based map of the water bodies. The methodology on how to make available the classified raster and vector based data will be presented in another study.

The generation of a vector data implies that all noisy pixels must be eliminated and a contextual reclassification of the seven classes. One proposal for noisy pixels is to remove all

isolated or clustered pixels and surrounded by non-water pixels only, if they do not meet a minimum size requirement. This proposal has the disadvantage of eliminating sections of small rivers with width just larger than the image sensor spatial resolution. For the contextual reclassification, the proposal is to reclassify a lower confidence class to a higher confidence one if the proportion of the shared edges is larger than a threshold. For example, if clustered pixels are from WATER50 class and share 30% of the edges with pixels classified as WATER60, and the proportion threshold is set to 30%, then they will be reclassified to WATER60. This reclassification process would be carried out from the lowest to the highest confidence class.

REFERENCES

- BLACKBRIDGE 2015. **Satellite Imagery Product Specifications**. Version 6.1: 1–48. Available at <http://www.blackbridge.com/rapideye/upload/RE_Product_Specifications_ENG.pdf>. Accessed in February, 2016.
- BOWKER, D. E.; R. E.; DAVIS, D. L. & MYRICK, K. STACY, & JONES, W. T. 1985. **Spectral Reflectances of Natural Targets for Use in Remote Sensing Studies**. NASA Reference Publication 1139. Available at <<http://ntrs.nasa.gov/search.jsp?R=19850022138>>. Accessed in April, 2016.
- CAMARA, G., SOUZA, R.C.M., FREITAS. U.M., GARRIDO, J. SPRING: Integrating remote sensing and GIS by object-oriented data modeling. **Computers & Graphics**, 20: (3) 395-403, May-Jun 1996.
- FOLEY, J. D., DAM, A. V., FEINER, S. K., & HUGHES, J. F. **Computer graphics: principles and practice**. New York: Addison-Wesley, 1996. 1264p.
- FRAZIER, P. S. & KENNETH, J. P. Water Body Detection and Delineation with Landsat TM Data. **Photogrammetric Engineering & Remote Sensing** 66 (12): 1461–67. 2000. doi:0099-1112I00I6612-1461\$3.00/0.
- MCFEETERS, S. K. The Use of the Normalized Difference Water Index (NDWI) in the Delineation of Open Water Features. **International Journal of Remote Sensing** 17 (7): 1425–32. 1996. doi:10.1080/01431169608948714.
- MMA. 2016. **Geo Catálogo Do Ministério Do Meio Ambiente**. Available at <<http://geocatalogo.mma.gov.br/sobre.jhtml>>. Accessed in November, 2015.
- NAMIKAWA, L. M. **Imagens landsat 8 para monitoramento de volume de água em reservatórios: estudo de caso nas barragens jaguari e jacareí do sistema cantareira**. In: Simpósio Brasileiro de Sensoriamento Remoto, 17. (SBSR), 2015, João Pessoa. Anais... São José dos Campos: INPE, 2015. p. 4828-4835. Internet. ISBN 978-85-17-0076-8.
- NOVO, E.M.M.; HANSOM, J.D. & CURRAN, P.J. The Effect of Sediment Type on the Relationship between Reflectance and Suspended Sediment Concentration. **International Journal of Remote Sensing** 10 (7): 1283–89. 1989. doi:10.1080/01431168908903967.
- RAPIDEYE. **Satellite Imagery Product Specifications**. Available at <http://www.rapideye.com/upload/RE_Product_Specifications_ENG.pdf>. Accessed in February, 2016.
- XU, H. 2006. Modification of Normalised Difference Water Index (NDWI) to Enhance Open Water Features in Remotely Sensed Imagery. **International Journal of Remote Sensing** 27 (14): 3025–33. doi:10.1080/0143116060058917.